

Calculation of incommensurability and spin excitations of diagonal stripes in underdoped lanthanum cuprates

G. Seibold¹ and J. Lorenzana²¹*Institut für Physik, BTU Cottbus, P.O. Box 101344, 03013 Cottbus, Germany*²*Dipartimento di Fisica, SMC-INFM and ISC, CNR, Università di Roma "La Sapienza," P. Aldo Moro 2, 00185 Roma, Italy*

(Received 6 July 2009; published 30 July 2009)

Based on the time-dependent Gutzwiller approximation we study the possibility that the diagonal incommensurate spin scattering in strongly underdoped lanthanum cuprates originates from antiferromagnetic domain walls (stripes). Calculation of the dynamic spin response for stripes in the diagonal phase yields the characteristic hour glass dispersion with the crossing of low-energy Goldstone and high-energy branches at a characteristic energy E_{cross} at the antiferromagnetic wave vector Q_{AF} . The high-energy part is close to the parent antiferromagnet. Our results suggest that inelastic neutron-scattering experiments on strongly underdoped lanthanum cuprates can be understood as due to a spatial mixture of bond-centered and site-centered stripe configurations with substantial disorder.

DOI: [10.1103/PhysRevB.80.012509](https://doi.org/10.1103/PhysRevB.80.012509)

PACS number(s): 74.25.Ha, 71.28.+d, 71.45.Lr, 74.72.Dn

The low-energy spin response of many high- T_c superconductors is characterized by magnetic fluctuations which are incommensurate with respect to the antiferromagnetic (AF) order (for a review see Ref. 1). Since in co-doped (with Eu, Nd, or Ba) lanthanum cuprates (LSCO) an accompanying charge-density wave has been detected (e.g., Ref. 2), this kind of scattering is usually attributed to the formation of stripe textures where the doped holes segregate into quasi-one-dimensional “rivers of charge” which simultaneously constitute domain walls for the AF order parameter.

The similarity of low-energy inelastic neutron-scattering (INS) data between co-doped and non-co-doped materials supports the picture of a fluctuating and (or) glassy stripe phase in LSCO. From these experiments it turns out that above doping $n_h=0.055$ the stripes are oriented along the Cu-O bond direction (“vertical stripes”) and the incommensurability δ (defined as the deviation of the magnetic peak from Q_{AF}) linearly increases up to $n_h \approx 1/8$.³ Above $n_h \approx 1/8$, δ stays essentially constant but the intensity of the low-energy spin fluctuations decreases and vanishes at the same concentration where superconductivity disappears in the overdoped regime, thus, suggesting an intimate relation between both phenomena.⁴

Upon lowering the doping below $n_h \approx 0.055$ the incommensurability δ rotates by 45° (Refs. 5–8) to the diagonal direction. Exactly at the same point superconductivity disappears; therefore to understand the nature of this diagonal phase is a key issue in the field.

The orthorhombic lattice distortion allows one to conclude that the elastic diagonal magnetic scattering is one-dimensional with the associated modulation along the orthorhombic b^* axis. When δ is measured in units of reciprocal tetragonal lattice units in both the vertical and diagonal phase, it turns out that the magnitude of the incommensurability numerically coincides across the rotation leading to a linear relation $\delta=x$. Upon approaching the border of the AF phase at $n_h=0.02$ the incommensurability approaches $\epsilon=x$,⁹ where ϵ is measured in units of reciprocal orthorhombic lattice units, thus $\epsilon=\sqrt{2}\delta$.

In this Brief Report we present computations of the incommensurability and the dynamic response of diagonal

stripes based on the Gutzwiller approximation and its dynamical extension and compare with our previous computations for vertical stripes and recent INS data.¹⁰ Our results suggest that in the spin-glass phase incommensurate scattering is due to a disordered spatial mixture of bond-centered and site-centered diagonal stripe configurations. Calculations are based on the one-band Hubbard model (on-site repulsion U) with hopping restricted to nearest ($\sim t$) and next-nearest ($\sim t'$) neighbors. Applying the unrestricted Gutzwiller approximation (GA) as in Ref. 11 static charge and spin textures are obtained by minimizing the corresponding energy functional. It has been shown¹² that for small clusters the charge distribution and energy obtained from this variational approach is in good agreement with density matrix renormalization group calculations,¹³ in contrast to the more conventional unrestricted Hartree-Fock approximation. In the present context it is, however, important that the GA can be implemented on sufficiently large clusters in order to obtain the desired information in momentum space.

Gaussian fluctuations are computed on top of the inhomogeneous solutions within the time-dependent GA (Refs. 14 and 15) (TDGA). This scheme allows for the calculation of random-phase-approximation (RPA) fluctuations in a similar manner as the traditional Hartree-Fock (HF) plus RPA. At the same time it starts from a solution which incorporates correlations already at mean-field level.

Parameters are $U/t=7.5$, $t'/t=-0.2$, and $t=340$ meV.¹⁶ In previous papers we have shown that our approach can reproduce both the magnon excitations of undoped LCO (Ref. 16) as revealed by neutron scattering¹⁷ and the doping-dependent incommensurability in the vertical stripe phase.^{12,18} In addition, the formalism leads to quantitative agreement with the dispersion of spin excitations in LBCO (Refs. 16, 19, and 20) and can reproduce the doping dependence of the optical conductivity.²¹

Figure 1 shows the charge and magnetization profile for the diagonal stripe structures we have obtained as stable saddle-point solutions within the GA. The first is a site centered diagonal (DSC) stripe where the doped holes are confined to nonmagnetic sites which simultaneously constitute the antiphase boundary for the AF order parameter.

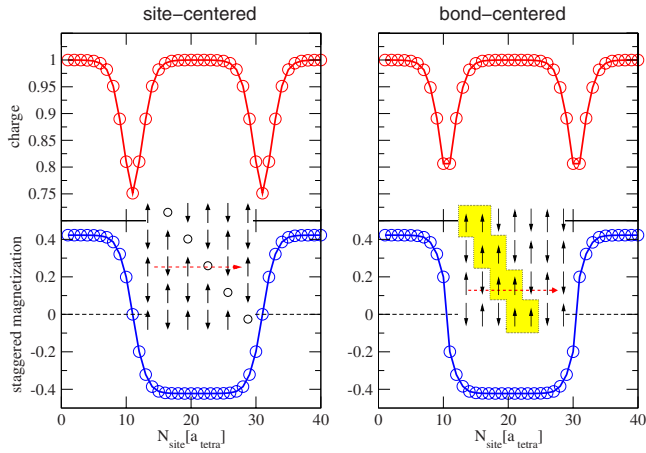


FIG. 1. (Color online) Charge density and magnetization for site-centered and bond-centered diagonal stripes. The densities are plotted along an horizontal scan, indicated by the dashed arrow.

The second stable texture (Fig. 1, right panel) can be considered as the diagonal counterpart to vertical bond-centered (VBC) stripes. However, due to the diagonal orientation the stripe acquires a net ferromagnetic moment. Moreover, the magnetization points in the same direction (i.e., the whole layer becomes ferromagnetic) when the BC stripes are separated by an odd number of lattice constants in x (or y) direction. They can be considered as the smallest “staircase” variant as discussed by Granath.²² More extended staircase structures can in principle not be excluded. However, due to the associated frustration at the corners of the staircase the ground state would display spin canting, which in our approach reflects as an instability in the transverse magnetic excitations.

The approximate linear relation between incommensurability and filling at low doping^{3,5–8} implies that isolated stripes are self-bounded linear aggregations of holes with a well-defined number of holes per Cu along the stripe given by $\nu_{opt} \equiv n_h/\epsilon$. Indeed as for vertical stripes^{12,18} we find an optimum filling; however, an important difference here is that ν_{opt} depends substantially on the texture. DSCs are insulating (the Fermi level falls in a gap) with $\nu_{opt} \approx 1$, thus $\epsilon \approx n_h$. Diagonal BC (DBC) stripes are metallic and have an optimum filling at $\nu_{opt} \approx 0.75$, implying $\delta \approx n_h$.²³

While DBC stripes are practically (accidentally) degenerate in energy with low doping VBC, the energy of the DSC texture is $\approx 0.02t$ per hole above.²³ We believe that these small energy differences are not significant given the simplicity of the model. A precise determination of the relative stability of the different phases would require at least multiorbital effects, inclusion of both long-range Coulomb interactions and coupling of the holes to the tilts of the CuO_4 octahedra. The latter have been shown to play a major role in the stabilization of vertical vs diagonal stripes.²⁴ On the other hand we believe that results within one phase are much more reliable. For example we have checked that the different optimum ν for DSC and DBC stripes for a three-band Hamiltonian do not differ from those found for the one-band model so that we consider this as a robust feature of our calculation.

In the present case the more important extrinsic effect is disorder. For vertical stripes the correlation length can reach

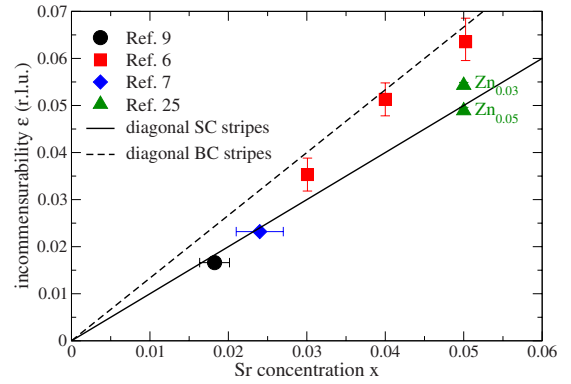


FIG. 2. (Color online) Doping dependence of the magnetic incommensurability ϵ in the diagonal phase as deduced from the referenced elastic neutron-scattering experiments. Solid and dashed lines are the predicted dependence for DSC and DBC stripes, respectively.

$150a_{tetra}$ or around 20 times the magnetic stripe periodicity, while for diagonal stripes the correlation is of the same order or even smaller than the periodicity.⁶ This should be kept in mind while comparing with our results which correspond to perfectly ordered stripes arrays. Figure 2 compares the doping dependence of the magnetic incommensurability ϵ in the diagonal phase as seen in elastic neutron-scattering experiments,^{6,7,9,25} together with the predicted dependence for DSC and DBC stripes. For non-co-doped samples the experimental incommensurability is in between the theoretical ones for DBC and DSC, with a stronger tendency for DBC close to the metal-insulator transition which shifts to DSC at low doping. An interesting effect occurs upon substitution of Cu^{2+} by nonmagnetic Zn^{2+} which has a filled $3d^{10}$ shell.²⁵ This should favor DSC stripes which are forced to have zero magnetic moments in the core, and indeed the incommensurability shifts to the computed DSC line (cf. Fig. 2) in accord with our expectation. All this suggests that the system is made of a disordered spatial mixture of DSC and DBC configurations with a gradual shift from the former to the latter as doping is increased.

In the following we discuss the spin excitations for doping $n_h=0.05$. For DSC stripes we have $\epsilon=0.05$ (i.e., charged stripes separated by $20a$ along the x or y direction) and for DBC stripes with $\epsilon=0.071$ (i.e., separated by $14a$ along x or y direction). Figure 3 displays $I(\omega, \mathbf{q}) \equiv \omega S(\omega, \mathbf{q})$ with $S(\omega, \mathbf{q})$ the transverse dynamical structure factor relevant for magnetic neutron-scattering experiments. The ω factor makes visible the high-energy features which would appear much faint in the experimentally accessible $S(\omega, \mathbf{q})$. We show the dispersions of magnetic excitations perpendicular (left panel) and parallel (right panel) to the stripe direction.

Parallel to the stripe the dispersion is dominated by modes very similar to the ones of the undoped AF, as could be expected from the real-space structure. Due to the large unit cell and the small extension of the reduced Brillouin zone in the perpendicular direction excitations consist of a large number of folded bands. These are generally silent when plotted in the extended Brillouin zone but acquire a large spectral weight in proximity to the modes of the parent antiferromagnet (shown with a dashed line), giving rise to the

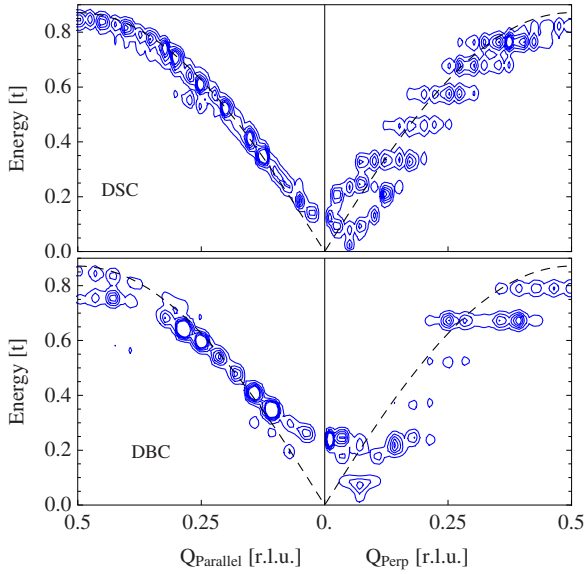


FIG. 3. (Color online) Magnetic excitations perpendicular and parallel to DSC (upper panel) and DBC (lower panel) stripes (doping $n_h=0.05$) as revealed by a contour plot with $I(\omega, \mathbf{q})=5, 10, 15, 20, 25$. The momentum scale is the distance from Q_{AF} measured in units of $2\pi/a_{ortho}$.

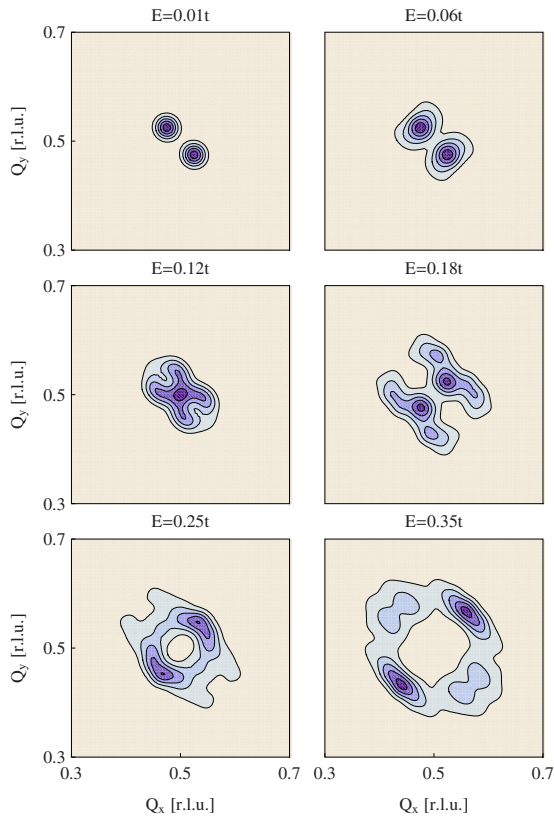


FIG. 4. (Color online) Constant frequency scans of $S(\omega, \mathbf{q})$ for DSC stripes ($n_h=0.05$, arbitrary intensity units). Data have been convoluted by a Gaussian in frequency and momentum space which half-width corresponds to the resolution of the calculation, i.e., $\delta\omega=0.01t$ and $\delta q=2\pi/801/a_{tetra}$. The center of each panel corresponds to Q_{AF} and wave vectors are denoted in units of $2\pi/a_{tetra}$.

horizontal segments in the right panel. This is analogous to the effect reported in photoemission where spectral weight is maximized when intersecting the free-electron dispersion relation.²² This clarifies the evolution of the spectrum at very low doping: As doping decreases the dynamical structure factor gradually tends to the one of the antiferromagnet by increasing the number of bands and modulating the spectral weight.

At low energies the spectrum is determined by the Goldstone excitations belonging to an inward (i.e., in the direction of $[\pi, \pi]$) and an outward dispersing branch. For DSC stripes upon increasing energy the inwards dispersing branch dominates in weight and reaches the AF wave vector Q_{AF} at $E_{cross} \approx 35$ meV, where it connects to the dispersion along the stripe. In contrast to the vertical excitations¹⁶ the saddle-point structure is very small and barely resolved due to finite-size effects. For DBC stripes a small gap appears between the Goldstone mode and the saddle point in strong resemblance with linear spin-wave theory (LSWT) results by Carlson *et al.*²⁶ There it was pointed out that for even spaced diagonal stripes (as in the present case) Q_{AF} becomes a reciprocal-lattice vector with a downturn of the acoustic branch. Interestingly for DSC stripes in our itinerant approach the analogous gap is not resolved, resulting in practice in a continuous dispersion of the Goldstone mode up to the saddle with energy E_{cross} . We expect that in both cases the gap will be washed out by disorder and damping effects.

In Fig. 4 we show cuts of the dispersion for the DSC stripes. At low frequencies the excitations at the two incommensurate wave vectors carry the dominant weight, which start to form spin-wave cones upon increasing energy. The cones merge at $E_{cross}=0.12t$ where it is apparent that the weight of the cones is strongly anisotropic and enhanced close to Q_{AF} . Similar to our previous findings for vertical stripes^{16,19} the response well above E_{cross} becomes two-

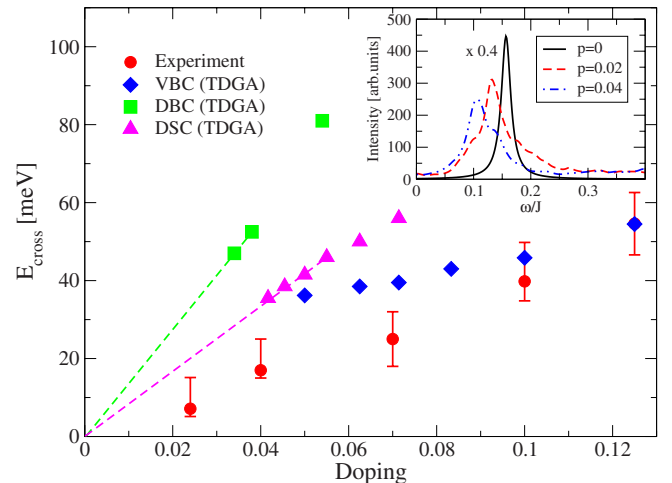


FIG. 5. (Color online) Doping dependence of E_{cross} for DSC and DBC stripes. Stars refer to results for vertical stripes and squares to diagonal ones. Circles with error bars are experimental data from Refs. 10 and 27–29. Dashed lines are the extrapolation of E_{cross} to $\omega=0$ at $n_h=0$. The inset depicts E_{cross} for various amounts of disorder (spin-flip probability p) for $\epsilon=0.055$ DBC stripes obtained within linear spin-wave theory.

dimensional, forming a ring shaped pattern around Q_{AF} .

Figure 5 reports the doping dependence of E_{cross} for both SC and BC textures in the vertical and diagonal phases compared to INS data.^{10,27–29} Since for the undoped system one recovers the spin excitations of the AF, E_{cross} extrapolates down to zero frequency at $n_h=0$ (dotted line) for both DSC and DBC stripes. Due to the large supercells involved we could not access the doping regime $n_h < 0.04$.

Below $x=0.08$ our computations overestimate E_{cross} . One should keep in mind that we are working with a fixed set of parameters determined in Ref. 16. For example reduction in t improves considerable the agreement but spoils the fitting of the undoped dispersion relation. Due to the complexity of the computations we have not performed intense optimization of the parameter set, so it may be that for different choices of U and t' and t we could also achieve a better fit of the overall doping dependence. However, we believe the main reason for the disagreement is the strong disorder character of the stripes in this doping range. We have performed linear spin-wave theory calculation of DBC stripes [nearest-neighbor exchange between antiferromagnetic ($\sim J$) and ferromagnetic ($\sim J'$) bonds] similar to Ref. 26 but including disorder by randomly flipping the spins (probability p). The inset to Fig. 5 demonstrates that already a small amount of disorder leads to a softening and broadening of E_{cross} . Indeed quite generally one expects a softening of excitations as the

magnetic configuration becomes more disordered. This becomes evident in the Ising limit, comparing the dispersion relation of an Ising ferromagnet (or AF) with that of an Ising spin glass in which the exchange constant J is the same but the sign is random. In the ordered case the spin-flip excitation energy is $2zJ$ with z the coordination, whereas in the glassy case it is smaller in average due to frustrated configurations. Based on a model of coupled spin-1/2 ladders the softening of magnetic excitations for disordered stripes has also been shown in Ref. 30.

To conclude, we have shown that the doping dependence of the incommensurability of diagonal magnetic scattering is compatible with a spatial mixture of DSC and DBC stripes. We find excitations that are qualitatively in accord with experiment¹⁰ but too high in energy. We attribute the difference to the much more disordered nature of diagonal incommensurate scattering. Our intermediate coupling approach predicts a quasi-two-dimensional high-energy response in the diagonal phase of LSCO which displays a one-dimensional static response along the orthorhombic b^* axis. Our computations also clarify how the dispersion relation converges to the one of the AF as doping is decreased.

We acknowledge support from the Vigoni Foundation and MIUR, PRIN 2007 (Protocol No. 2007FW3MJX003).

- ¹J. M. Tranquada, in *Handbook of High-Temperature Superconductivity*, edited by J. R. Schrieffer (Springer, Heidelberg, 2007).
- ²P. Abbamonte, A. Rusydi, S. Smadici, G. D. Gu, G. A. Sawatzky, and D. L. Feng, *Nat. Phys.* **1**, 155 (2005).
- ³K. Yamada, C. H. Lee, K. Kurahashi, J. Wada, S. Wakimoto, S. Ueki, H. Kimura, Y. Endoh, S. Hosoya, G. Shirane, R. J. Birgeneau, M. Greven, M. A. Kastner, and Y. J. Kim, *Phys. Rev. B* **57**, 6165 (1998).
- ⁴S. Wakimoto, H. Zhang, K. Yamada, I. Swainson, Hyunkyung Kim, and R. J. Birgeneau, *Phys. Rev. Lett.* **92**, 217004 (2004).
- ⁵S. Wakimoto, G. Shirane, Y. Endoh, K. Hirota, S. Ueki, K. Yamada, R. J. Birgeneau, M. A. Kastner, Y. S. Lee, P. M. Gehring, and S. H. Lee, *Phys. Rev. B* **60**, R769 (1999).
- ⁶S. Wakimoto, R. J. Birgeneau, M. A. Kastner, Y. S. Lee, R. Erwin, P. M. Gehring, S. H. Lee, M. Fujita, K. Yamada, Y. Endoh, K. Hirota, and G. Shirane, *Phys. Rev. B* **61**, 3699 (2000).
- ⁷M. Matsuda, M. Fujita, K. Yamada, R. J. Birgeneau, M. A. Kastner, H. Hiraka, Y. Endoh, S. Wakimoto, and G. Shirane, *Phys. Rev. B* **62**, 9148 (2000).
- ⁸M. Fujita, K. Yamada, H. Hiraka, P. M. Gehring, S. H. Lee, S. Wakimoto, and G. Shirane, *Phys. Rev. B* **65**, 064505 (2002).
- ⁹M. Matsuda, M. Fujita, K. Yamada, R. J. Birgeneau, Y. Endoh, and G. Shirane, *Phys. Rev. B* **65**, 134515 (2002).
- ¹⁰M. Matsuda, M. Fujita, S. Wakimoto, J. A. Fernandez-Baca, J. M. Tranquada, and K. Yamada, *Phys. Rev. Lett.* **101**, 197001 (2008).
- ¹¹G. Seibold, E. Sigmund, and V. Hizhnyakov, *Phys. Rev. B* **57**, 6937 (1998).
- ¹²G. Seibold and J. Lorenzana, *Phys. Rev. B* **69**, 134513 (2004).
- ¹³S. R. White and D. J. Scalapino, *Phys. Rev. Lett.* **91**, 136403 (2003).
- ¹⁴G. Seibold and J. Lorenzana, *Phys. Rev. Lett.* **86**, 2605 (2001).
- ¹⁵G. Seibold, F. Becca, P. Rubin, and J. Lorenzana, *Phys. Rev. B* **69**, 155113 (2004).
- ¹⁶G. Seibold and J. Lorenzana, *Phys. Rev. B* **73**, 144515 (2006).
- ¹⁷R. Coldea, S. M. Hayden, G. Aeppli, T. G. Perring, C. D. Frost, T. E. Mason, S.-W. Cheong, and Z. Fisk, *Phys. Rev. Lett.* **86**, 5377 (2001).
- ¹⁸J. Lorenzana and G. Seibold, *Phys. Rev. Lett.* **89**, 136401 (2002).
- ¹⁹G. Seibold and J. Lorenzana, *Phys. Rev. Lett.* **94**, 107006 (2005).
- ²⁰J. Lorenzana, G. Seibold, and R. Coldea, *Phys. Rev. B* **72**, 224511 (2005).
- ²¹J. Lorenzana and G. Seibold, *Phys. Rev. Lett.* **90**, 066404 (2003).
- ²²M. Granath, *Phys. Rev. B* **69**, 214433 (2004).
- ²³G. Seibold and J. Lorenzana, arXiv:0907.5174 (unpublished).
- ²⁴B. Normand and A. P. Kampf, *Phys. Rev. B* **64**, 024521 (2001).
- ²⁵M. Matsuda, M. Fujita, and K. Yamada, *Phys. Rev. B* **73**, 140503(R) (2006).
- ²⁶E. W. Carlson, D. X. Yao, and D. K. Campbell, *Phys. Rev. B* **70**, 064505 (2004).
- ²⁷M. Kofu, T. Yokoo, F. Trouw, and K. Yamada, arXiv:0710.5766 (unpublished).
- ²⁸J. M. Tranquada, H. Woo, T. G. Perring, H. Goka, G. D. Gu, G. Xu, M. Fujita, and K. Yamada, *Nature (London)* **429**, 534 (2004).
- ²⁹H. Hiraka, Y. Endoh, M. Fujita, Y. S. Lee, J. Kulda, A. Ivanov, and R. J. Birgeneau, *J. Phys. Soc. Jpn.* **70**, 853 (2001).
- ³⁰B. M. Andersen and O. F. Syljuåsen, *Phys. Rev. B* **75**, 012506 (2007).